

# New Trends in Designing Parabolic trough Solar Concentrators and Heat Storage Concrete Systems in Solar Power Plants

Valentina A. Salomoni<sup>1</sup>, Carmelo E. Majorana<sup>1</sup>, Giuseppe M. Giannuzzi<sup>2</sup>,  
Adio Miliozzi<sup>2</sup> and Daniele Nicolini<sup>2</sup>

<sup>1</sup>*University of Padua*

<sup>2</sup>*ENEA – Agency for New Technologies, Energy and Environment  
Italy*

## 1. Introduction

Energy availability has always been an essential component of human civilization and the energetic consumption is directly linked to the produced wealth. In many depressed countries the level of solar radiation is considerably high and it could be the primary energy source under conditions that low cost, simple-to-be-used technologies are employed. Then, it is responsibility of the most advanced countries to develop new equipments to allow this progress for taking place. A large part of the energetic forecast, based on economic projection for the next decades, ensure us that fossil fuel supplies will be largely enough to cover the demand. The predicted and consistent increase in the energetic demand will be more and more covered by a larger use of fossil fuels, without great technology innovations. A series of worrying consequences are involved in the above scenario: important climatic changes are linked to strong CO<sub>2</sub> emissions; sustainable development is hindered by some problems linked to certainty of oil and natural gas supply; problems of global poverty are not solved but amplified by the unavoidable increase in fossil fuel prices caused by an increase in demand. These negative aspects can be avoided only if a really innovative and more acceptable technology will be available in the next decades at a suitable level to impress a substantial effect on the society. Solar energy is the ideal candidate to break this vicious circle between economic progress and consequent greenhouse effect. The low penetration on the market shown today by the existent renewable technologies, solar energy included, is explained by well-known reasons: the still high costs of the produced energy and the “discontinuity” of both solar and wind energies. These limitations must be removed in reasonable short times, with the support of innovative technologies, in view of such an urgent scenario.

On this purpose ENEA, on the basis of the Italian law n. 388/2000, has started an R&D program addressed to the development of CSP (*Concentrated Solar Power*) systems able to take advantage of solar energy as heat source at high temperature. One of the most relevant objectives of this research program (Rubbia, 2001) is the study of CSP systems operating in the field of medium temperatures (about 550°C), directed towards the development of a new and low-cost technology to concentrate the direct radiation and efficiently convert solar

Source: Solar Energy, Book edited by: Radu D. Rugescu,  
ISBN 978-953-307-052-0, pp. 432, February 2010, INTECH, Croatia, downloaded from SCIYO.COM

energy into high temperature heat; another aspect is focused on the production of hydrogen by means of thermo-chemical processes at temperatures above 800°C.

As well as cost reductions, the current innovative ENEA conception aims to introduce a set of innovations, concerning: i) *The parabolic-trough solar collector*: an innovative design to reduce production costs, installation and maintenance and to improve thermal efficiency is defined in collaboration with some Italian industries; ii) *The heat transfer fluid*: the synthetic hydrocarbon oil, which is flammable, expensive and unusable beyond 400°C, is substituted by a mixture of molten salts (sodium and potassium nitrate), widely used in the industrial field and chemically stable up to 600°C; iii) *The thermal storage (TES)*: it allows for the storage of solar energy, which is then used when energy is not directly available from the sun (night and covered sky) (Pilkington, 2000). After some years of R&D activities, ENEA has built an experimental facility (defined within the Italian context as PCS, “*Prova Collettori Solari*”) at the Research Centre of Casaccia in Rome (ENEA, 2003), which incorporates the main proposed innovative elements (Figure 1). The next step is to test these innovations at full scale by means of a demonstration plant, as envisioned by the “*Archimede*” ENEA/ENEL Project in Sicily. Such a project is designed to upgrade the ENEL thermo-electrical combined-cycle power plant by about 5 MW, using solar thermal energy from concentrating parabolic-trough collectors.



Fig. 1. PCS tool solar collectors at ENEA Centre (Casaccia, Rome).

Particularly, the Chapter will focus on points i) and iii) above:

- loads, actions, and more generally, the whole design procedure for steel components of parabolic-trough solar concentrators will be considered in agreement with the Limit State method, as well as a new approach will be critically and carefully proposed to use this method in designing and testing “special structures” such as the one considered here;
- concrete tanks durability under prolonged thermal loads and temperature variations will be estimated by means of an upgraded F.E. coupled model for heat and mass transport (plus mechanical balance). The presence of a surrounding soil volume will be additionally accounted for to evaluate environmental risk scenarios.

Specific technological innovations will be considered, such as:

- higher structural safety related to the reduced settlements coming from the chosen shape of the tank (a below-grade cone shape storage);
- employment of HPC containment structures and foundations characterized by lower costs with respect to stainless steel structures;
- substitution of highly expensive corrugated steel liners with plane liners taking advantage of the geometric compensation of thermal dilations due to the conical shape of the tank;
- possibility of employing freezing passive systems for the concrete basement made of HPC, able to sustain temperature levels higher than those for OPC;
- fewer problems when the tank is located on low-strength soils.

## 2. Description of parabolic-trough solar concentrators

The parabolic-trough solar concentrators are one of the basic elements of a concentrating solar power plant. The functional thermodynamic process of a solar plant is shown in (Herrmann et al., 2004). The main elements of the plant are: the solar field, the storage system, the steam generator and the auxiliary systems for starting and controlling the plant. The solar field is the heart of the plant; the solar radiation replaces the fuel in conventional plants and the solar concentrators absorb and concentrate it. The field is made up of several collector elements composed in series to create the single collector line. The collected thermal energy is determined by the total number of collector elements which are characterized by a reflecting parabolic section (the concentrator), collecting and continuously concentrating the direct solar radiation by means of a sun-tracking control system to a linear receiver located on the focus of the parabolas. A circulating fluid flows inside a linear receiver to transport the absorbed heat.

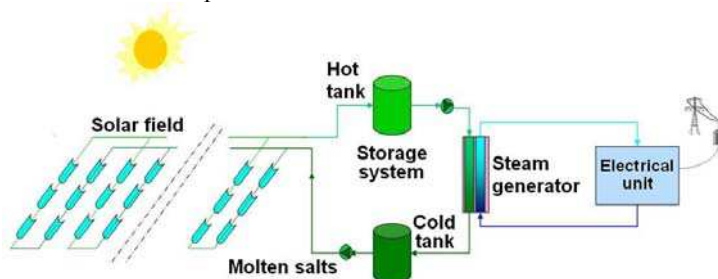


Fig. 2. Functional thermodynamic process flow of a solar plant.

A solar parabolic-trough collector line is divided into two parts from a central pylon supporting the hydraulic drive system (Antonaia et al., 2001). Each part is composed by an equal number of identical collector elements, connected mechanically in series. Each collector element consists of a support structure for the reflecting surfaces, the parabolic mirrors, the receiver line and the pylons connecting the whole system to a solid foundation by means of anchor bolts. The configuration of a solar parabolic-trough collector is that of a cylindrical-parabolic reflecting surface with a receiver tube co-axial with the focus-line, as a first approximation. The reflecting surface must be able to rotate around an axis parallel to the receiver tube, to constantly ensure that the incident radiation and the plane containing the parabolic sections' axes are parallel. In this way the incident solar light on the reflecting

surfaces is concentrated and continuously intercepted by the receiver tube in any assumed position of the sun during its apparent motion. The parabolic-trough collector is then constituted by a rotating "mobile part" to orientate the concentrator reflecting surfaces and by a "fixed part" guaranteeing support and connection to the ground of the mobile part.

The solar collector performances, in terms both of mechanical strength and optical precision, are related to one side to the structural stiffness and on the other to the applied load level. The main load for a solar collector is that coming from the wind action on the structure and it is applied as a pressure distributed on the collector surfaces.

From a structural point of view, it must be emphasized that the parabolic-trough concentrator is composed mainly by three systems: the *concentration*, the *torque* and the *support system*. Other fundamental elements, not treated in this document for sake of brevity, are the *foundation* and the *motion systems*. In Table 1 the subsystems and basic elements characterizing the structure of the concentrator developed by ENEA are shown. All elements should be considered when designing a parabolic-trough concentrator and verified for "operational" and "survival" load conditions. Corrosion risks and safe-life (about 25-30 years) must be taken into account as well.

The following basic operational conditions, listed in Table 2, can be considered valid for a parabolic-trough concentrator; they define different performance levels under wind conditions. "Design conditions" can be fixed consequently.

Finally, on the basis of what described above, the main requirements when designing a parabolic-trough concentrator can be summarized as follows:

- *Safety*: the collector structures exposed to static loads must guarantee adequate safety levels to ensure public protection, according (in our case) to the Italian Law 1086/71. This is translated into a suitable strength level or more generally in safety factors for the construction within the *Limit State Analysis*.
- *Optical performance*: the structure must guarantee a suitable stiffness in order to obtain, under operational conditions, limited displacements and rotations, the optical performance level being related to the capacity of the mirrors concentrating the reflected radiation on the receiver tube.
- *Mechanical functionality*: the structural adaptation to loads must not produce interference among mobile and fixed parts of the structure under certain load conditions.
- *Low cost*: the structure has to respond to typical economic requirements for solar plant fields (e.g. known from experiences abroad): unlimited plant costs lead to non-competitive sources employments. This can lead to tolerate fixed damage levels of the structure under extreme conditions (i.e. collapse of not-bearing elements, local yield, etc.), but still respecting the above mentioned requirements of public protection.

### 3. Codes of practice and rules

The parabolic-trough concentrator, on the basis of its structural shape and use and further considering available National and European recommendations, is classifiable as a "special structure" (Majorana & Salomoni, 2004 (a); Giannuzzi et al., 2007): it is not a machine or a standard construction. The definition "special" comes directly from a subdivision in classes and categories according to the criterion of the "Rates for professional services" as it results from the Italian law n. 143/1949; this law places "Metallic structures of special type, notable constructive importance and requiring ad-hoc calculations" into class IX e subclass b.

Systems	Subsystems	Elements
<i>Concentration system</i>	Reflecting surfaces	Mirrors, Mirror-structure connection
	Mirrors support structures	Girders, Girder-framed structure connection Framed structure, Framed structure-torque tube connection
<i>Torque system</i>	Torque tube, plate, hinge	Torque tube, Torque tube-plate connection, Plate, Plate-hinge connection, Hinge
<i>Module supports</i>	Intermediate / final pylons	Cylindrical pin joint, Pin joint-support connection, Framed structure, Plate, Anchor bolts
	Central pylon	Cylindrical pin joint, Pin joint-support connection, Framed structure, Engine support structure, Plate, Anchor bolts
<i>Other</i>	Foundations	Piles and/or plinths, Anchor bolts
	Drive system	Hydraulic drive/pistons, etc.

Table 1. Example of structural elements of a parabolic-trough concentrator.

<i>Level</i>	<i>Condition</i>
<b>W1</b>	Response under normal operational conditions with light winds. The concentration efficiency must be as high as possible under wind velocity less than a value $v_1$ characterizing this level.
<b>W2</b>	Response under normal operational conditions with medium winds. The concentration efficiency is gradually diminishing under wind velocity comprised between $v_1$ and $v_2$ . The wind velocity $v_2$ characterizes this level.
<b>W3</b>	Transition between normal operating conditions and survival positions under medium-to-strong or strong winds. The survival must be ensured in any position under medium-strong winds. The drive must be able to take the collector to safe positions for any wind velocity comprised between $v_2$ and $v_3$ . The wind velocity $v_3$ characterizes this level.
<b>W4</b>	Survival under strong winds in "rest" positions. The survival wind velocity must be adapted to the requests of the site according to recommendations. The wind velocity $v_4$ characterizes this level.

Table 2. Operational conditions.

From the functional analysis of the structure its special typology clearly emerges, according to its design, technical arrangements and innovation. When the parabolas are stopped in an assigned angular configuration, the nature of the structure can be determined: steel structure of mixed type founded on simple or reinforced concrete placed on a foundation

soil having characteristics closely correlated to a chosen site, also under the seismic profile. From the structural point of view, the dynamic characteristics play a major role, with the response deeply influenced not only by the drive-induced oscillations, but also by dominant winds or seismic actions. Taking into account the above considerations, it is then possible to state that the examined structure is “*special*”.

Moreover, such a structure requires appropriate calculations since some parts are mobile, even if with a slow rotation; at the same time the structure is subjected to wind actions, especially relevant due to the parabolas dimension. The simultaneous thermal and seismic actions, acting as self-equilibrated stresses in an externally hyperstatic structure, are equally important. Special steel made structures are e.g. cranes: they are designed using specific recommendations; in our case the reference to existing codes of practice is necessary, even if with the aim of adapting them and/or proposing new ones for CSP systems. Hence it clearly appears that such structures, built within the European countries, are currently designed and verified out of standards; the only two Italian recommendations acting as guidelines are:

- Law 5/11/71, n.1086, Norms to discipline the structures made by plain and pre-stressed reinforced concrete and by metallic materials.
- Law 2/2/74, n.64, Procedures devoted to structures with special prescriptions for seismic zones.

Moreover, several “technical norms” are related to the above ones, in form of “Minister (of Public Works) Decrees”, or “explanation documents”, or other documents giving rise to a certain amount of duplications and repetitions; however, a progressive compulsory use of Eurocodes is being introduced to push Italian engineers more properly into the European environment. In this case, Eurocodes 3 and 8 are of interest for the structural design of solar concentrators, also in view of their seismic performance. It is important to make an advanced choice regarding the body of recommendations to be followed in the design and checking phases and to proceed further with them, avoiding the common mistake of some designers to take parts from one norm (i.e. Italian) and mix it with parts of another norm (i.e. Eurocodes). The main problems in the so-called harmonization of rules within Europe reside in finding safety coefficients to be applied for considering special conditions (e.g. environmental) in each country, as well as those for materials. This is a source of difficulty in the creation of a unique body of rules valid in the whole European territory. The last product of recommendations recently emitted by the actual Ministry of Public Works in Italy is a 438 pages document (plus two Annexes) named “*Testo Unico per le Costruzioni*”. It is compulsory in the Italian territory from July 1<sup>st</sup> 2009. The aim of this decree was also to unify a series of previous decrees into a single document. As already stated, it has been here chosen to follow the current Italian laws, and Eurocodes for comparison, in view of the possible application of solar concentrators at Priolo Gargallo (near Syracuse, Sicily). In principle, with a few changes, it is possible to apply the technology in other sites, as well as outside Italy or even Europe: slight changes in dimensioning could occur.

Hence, to take into account the specificity of the investigated structures, it was necessary to combine together *operational states* (OSs) (Table 2), *characteristic positions* and *load actions*, reaching to the interpretation of Table 3 within the context of a *limit state* (LS) analysis (Salomoni et al., 2006). Additionally, within the *serviceability limit states* (SLSs) the conditions of maximum rotation ( $W_1$  operational state) and maximum deformation ( $W_2$ ) must be verified;  $W_3$  requires the collector operability within an elastic *ultimate limit state* (ULS), i.e. absence of permanent deformations. Differently, such deformations can be present within  $W_4$  but without leading to a structural collapse.

Characteristic positions			-120°	-30°	0°	30°	60°	75°
Operational states								
$v_{ref}$ [m/sec]	↓	Limit state						
7	W <sub>1</sub>	SLS		Y				
14	W <sub>2</sub>	SLS					Y	
21	W <sub>3</sub>	ULS	Y	Y	Y	Y	Y	Y
28	W <sub>4</sub>	ULS	Y		Y			

Table 3. Example of combinations among characteristic positions, operational states and load actions to study CSPs in the context of LS analyses.

### 4. Materials

The solar concentrator supporting structure is made of hot-laminated steel. Hence, according to Eurocode 3 and UNI EN 10025, steels in form of bars, plates or tubes must be of the types shown in Table 4.

However recommendations allow for using different types of steel once the ensured safety level remains the same, justifying this through appropriate theoretical and experimental documentations. Under uniaxial stress states, their design strengths can be deduced from tables; in case of multiaxial states, suitable combinations are additionally given. In our calculations, the following material characteristics are considered: elastic modulus  $E = 210000 \text{ N/mm}^2$ , Poisson’s coefficient  $\nu = 0.3$ , thermal expansion coefficient  $\alpha = 12 \cdot 10^{-6} \text{ }^\circ\text{C}^{-1}$  and density  $\rho = 7850 \text{ kg/m}^3$ . If welding is used for connecting elements, the behaviour of steel types S235 and S275 is distinguished from that of S360.

Nominal steel type	thickness t [mm]			
	t ≤ 40		40 < t ≤ 100	
	$f_y$ [N/mm <sup>2</sup> ]	$f_u$ [N/mm <sup>2</sup> ]	$f_y$ [N/mm <sup>2</sup> ]	$f_u$ [N/mm <sup>2</sup> ]
Fe360 / S235 (EN 10025)	235	360	215	340
Fe430 / S275 (EN 10025)	275	430	255	410
Fe510 / S360 (EN 10025)	360	510	335	490

Table 4. Strengths and failure stresses (nominal values) for structural steels.

### 5. Loads

Given the design loads, subdivided in *permanent* and *variable* ones, wind conditions are here examined more in detail, whose effects on the structure are connected to the parabolas aerodynamics in their different characteristic positions (see below). The role of the snow has been additionally considered.

## 5.1 Variable loads

### 5.1.1 Wind action on the paraboloids

The mean value of wind velocity, as a function of the distance from soil  $V_m(z)$ , is expressed by

$$V_m(z) = C_r(z) \cdot C_t(z) \cdot V_{ref} \quad (1)$$

where  $V_{ref}$  is the reference wind velocity,  $C_r(z)$  the roughness coefficient and  $C_t(z)$  the topographic coefficient.

The reference wind velocity  $V_{ref}$  is defined as the mean wind speed over a time period of 10 min, at 10 m height on a second category soil, with a 50 years "return period". The reference wind speeds for each Italian area is given by recommendations; e.g. a site located near the sea in Southern Italy has a reference wind speed of about 28 m/s. An important wind speed value is the peak wind speed which can be seen as the superposition of the mean wind speed plus its variation due to turbulence conditions on site. It can be evaluated as

$$V_{peak}(z) = G(z) \cdot V_m(z) \quad (2)$$

where  $G(z)$  is the "peak factor", that is,

$$G = \sqrt{1 + \frac{7}{C_t(z) \cdot \ln(z/z_0)}} \quad (3)$$

Usually  $G$  is comprised between 1.5 and 1.6. It should be emphasized that the check under failure loads must be necessarily performed on the basis of the peak velocity, since this gives an overload capable of making the material reach its strength limit, even if its duration is short. As far as the operational performance is concerned, it is more feasible to use the mean velocity. The roughness coefficient  $C_r(z)$  takes into account the variability of the mean wind speed and the site characteristics by considering the height over the soil and the soil roughness as functions of the wind direction. The roughness coefficient at height  $z$  is defined by the logarithmic profile

$$C_r(z) = k_r \ln(z/z_0) \quad (4)$$

where  $k_r$  is the soil factor and  $z_0$  is the roughness length, both related to the soil exposure category on its turn linked to the geographic location of the investigated area within Italy and on the basis of the soil roughness. In case of an open country,  $k_r$  is 0.19 and  $z_0$  is 0.05 m. The topographic coefficient  $C_t(z)$  takes into account the increment in the mean wind speed on escarpments and isolated hills; in our case  $C_t = 1$  can be taken.

The solar concentrator shape is taken into account by means of aerodynamic coefficients. The different aerodynamic shape coefficients have been identified by means of a CFD analysis carried out in (Miliozzi et al., 2007). These coefficients have been determined starting from wind actions exerted on the linear parabolic collector as functions of its angular position (Figure 3). Such coefficients have been calculated for the most (external) and the least (internal) stressed collectors (Giannuzzi, 2007), see e.g. Figure 4. An external collector is one of those belonging to the first line without any artificial barrier against wind actions, whereas an internal collector is one on the sixth line, taken as representative of all the others.



Full tables for shape coefficients in case of “external” parabolas as well as “internal” ones are reported in (Majorana & Salomoni, 2005 (a)) and used in (Majorana & Salomoni, 2005 (b)) for structural assessment within the Limit State Design. Shape coefficients have been used to evaluate drag ( $C_{fx}$ ), lift ( $C_{fy}$ ), torsion ( $C_{Mz}$ ) and mean pressure ( $C_{pm}$ ), each of them being function of the concentrator rotation angle, where the allowed rotation is in the range  $\pm 120^\circ$ . Then, shape coefficients for mean pressures have been calculated as functions of the aperture angle for “external” or “internal” parabolas. By analyzing the above coefficients it is possible to identify the parabolas’ characteristic positions listed in Table 5.

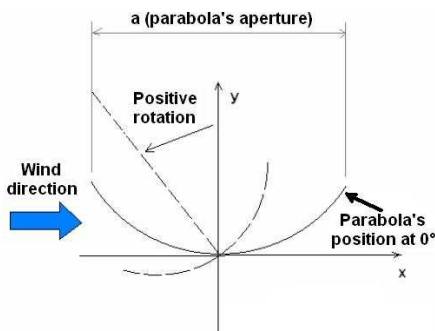


Fig. 3. Parabolic concentrator scheme at different angular positions.

Starting from the calculated shape coefficients, the corresponding effects referring to drag and lift force, torsion, mean pressure and pressure distribution have been determined. By analyzing the results of the CFD analysis, it has been evidenced that aerodynamic coefficients and associated loads are largely reduced at the internal collectors. The main reason resides in the shielding effect produced by the first collectors’ rows. This remark leads to the necessity of designing “strong” collectors along the external rows (Figure 4) and “light” collectors along the internal ones. Alternatively, it is possible to choose a different

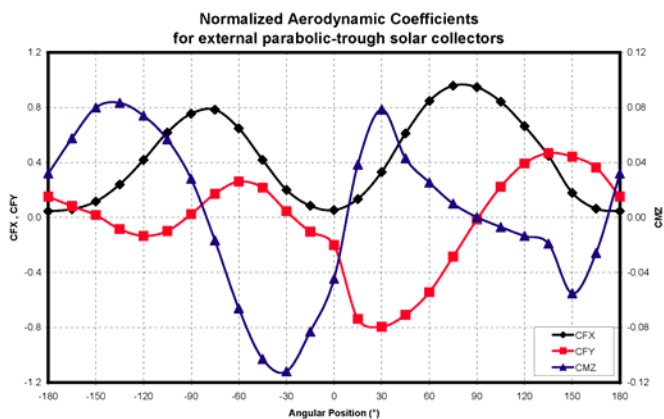


Fig. 4. Angular distribution of the normalized shape coefficients for “external” parabolas.

design strategy, based on the introduction of opportune windbreak barriers and on the realization of "light" collectors only. The position characterized by smaller loads is at 180°. This is only a theoretical, unattainable position because of the interferences between receivers and pylons. The safety position to be really taken in consideration is at about -120°. The waiting position (at 0°) does not guarantee an adequate level of protection for the mirrors. All the positions shown in Table 5 must be taken into account during the design phase but the most relevant position is, without doubt, the one associated to the maximum torque action. This is consequence of the fact that torque effects are accumulated along all the line, producing the maximum stresses on the structural elements close to the central pylon. This can be considered the key action in the parabolic-trough solar concentrators wind design.

### 5.1.2 Snow

The snow load is usually evaluated on the roofs (here parabolas), by means of the following expression

$$q_s = \mu_i \cdot q_{sk} \quad (5)$$

where  $q_s$  is the snow load on the roof,  $\mu_i$  the roof shape coefficient and  $q_{sk}$  the reference value of the snow load on the ground.

Characteristic Effect	Angular position (degrees)	
	"External" collector	"Internal" collector
<i>Safety position</i>	-120	-120
<i>Waiting position</i>	0	0
<i>Maximum torque effect</i>	-30	-15
<i>Maximum bending action on the torque tube</i>	+60	+30
<i>Maximum drag force</i>	+75	-45
<i>Maximum lift force</i>	+120	-45
<i>Maximum crush force</i>	+30	+30

Table 5. Wind effect: characteristic positions.

The load acts along the vertical direction and it is referred to the horizontal projection of the covering surface. The snow load on the ground depends on local environmental and exposure conditions, where the variability of the snowfall from region to region is taken into account. The reference snow load in locations at heights less than 1500 m over the mean sea level (m.s.l.) has to be evaluated on the basis of given expressions (whose values correspond to a "return period" of about 200 years). In case of a region like Sicily and a site located at a reference height less then 200 m m.s.l.,  $q_{sk}$  is about 0.75 kN/m<sup>2</sup>. The shape coefficients to be used for the snow load are those indicated in Table 6, being  $\alpha$  (degrees) the angle between cover and the horizontal plane.

The shape coefficients  $\mu_1$ ,  $\mu_2$ ,  $\mu_3$ ,  $\mu_{1^*}$  refer to roofs having one or more slopes, and they should be evaluated as functions of  $\alpha$ , as indicated by the codes. For given parabolas positions, other coefficients can be used, as e.g. those related to cylindrical covers. In absence of rifting inhibiting snow sliding, for cylindrical covers of any shape and single

curvature of constant sign, the worst uniform and not-symmetric load distribution is there considered.

	$0^\circ \leq \alpha \leq 15^\circ$	$15^\circ < \alpha \leq 30^\circ$	$30^\circ < \alpha \leq 60^\circ$	$\alpha > 60^\circ$
$\mu_1$	0.8	0.8	$0.8(60-\alpha)/30$	0.0
$\mu_2$	0.8	$0.8+0.4(\alpha-15)/30$	$(60-\alpha)/30$	0.0
$\mu_3$	$0.8+0.8\alpha/30$	$0.8+0.8\alpha/30$	1.6	-
$\mu_1^*$	0.8	$0.8(60-\alpha)/45$		0

Table 6. Shape coefficient for the snow load (Eurocode1-Part 2.3).

In our case, to determine the shape coefficients  $\mu_i$  for the parabolas, it is possible to approximatively evaluate the maximum slope of the parabolic collector with respect to the horizontal line, if it is rotated with its concavity upwards, being the element profile defined by means of the equation

$$y = x^2 / 4f \tag{6}$$

where  $-2950 < x < 2950$  (mm),  $f = 1810$  (mm); and the slope by

$$y' = x / 2f \tag{7}$$

with maximum value equal to 0.815, corresponding to an angle  $\alpha$  such that  $\text{tg}\alpha = 0.815$ , i.e.  $\alpha \approx 39^\circ$ . On the other side, taking into account the value corresponding to  $x/2$ , then  $\alpha = 22^\circ$ . Hence, assuming  $\alpha = 22^\circ$  as a mean value, it is possible to calculate the shape coefficients as indicated in the recommendations. The corresponding load conditions are shown in Figure 5.

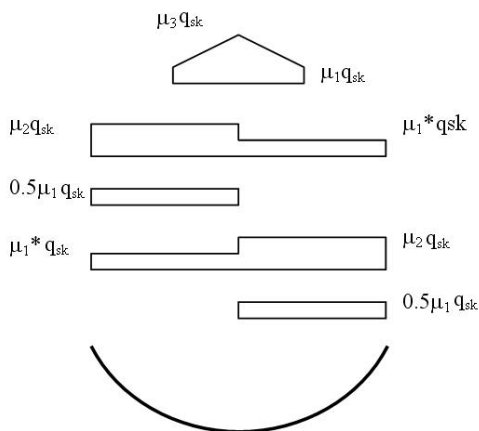


Fig. 5. Snow conditions for the parabolas when the solar collector is rotated to the waiting position.

As demonstrated in (Majorana & Salomoni, 2005 (b)), snow effects are fundamental when verifying the structure in the safety position (Table 5) or when seismic effects are included.

Discussing about the real significance of such an effect when considering desert locations (as those typical for CSP systems) is reasonable: this should be another example of the necessity for ad-hoc codes of practice when studying *special* structures in possibly *special* sites.

The parabola's configuration with its concavity upwards (Figure 5) is not the only possible one when evaluating the effects of the snow; being the snowy phenomenon largely predictable, so that a rotation of the collector towards the safety position is expected, an additional investigated angular position for analyzing snow effects refers to  $\alpha = \pm 120^\circ$ . When e.g.  $\alpha = +120^\circ$ , the situation is the one of Figure 6; the remaining characteristic positions, even associable to different OSs, can be considered as characterized by a null snow action: in fact, in case of snow, the collector would be evidently moved to its safety position with no tracking. Additionally, being  $L_1$  (distance between the point, on the rotated parabola, with null tangent and the origin of the vertical axis)  $> L$  ( $= 2950$  mm in our case), it is precautionarily assumed  $L_1 = L$  and hence from Eurocodes  $\mu_1 = 0.8$ ,  $\mu_2 = 2.0$  ( $\mu_3 = 1.0$ ), with loads as those of Figure 7.

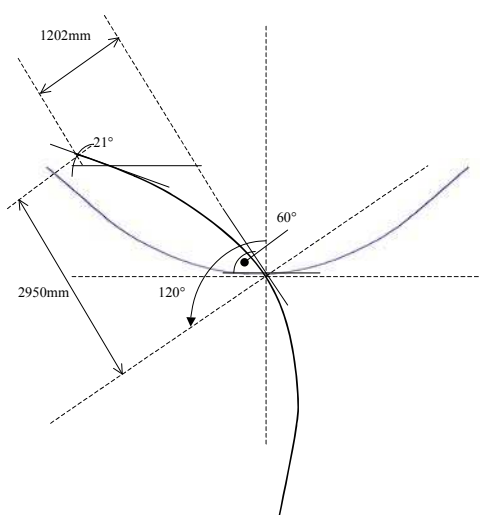


Fig. 6. Parabola's position for evaluating snow effects.

Two changes have been essentially introduced to what indicated by the codes: being, as already stated,  $L_1 > L$ , the point of null load amplified by  $\mu_2$  goes outside the effective parabola's projected dimension (consequently, the effect of  $\mu_3$  is zero; anyway, we are still in favour of safety being  $\mu_2 > \mu_3$ ) and this explains the chosen trapezoidal shape for the load of Figure 7; the load cusp (from Eurocodes falling on the point whose slope on the curve is of  $30^\circ$ , i.e. at  $L_1/4$ ), considered the not-symmetric parabolic profile, is moved with respect to  $L_1/4$ .

Then, when combining the loads, among the various indicated load conditions only those revealed as heaviest for the structural system have been adopted.

Hence, the main load combinations are reported in Table 7, where the multiplicative coefficients related to each basic action (permanent,  $G_k$ , and variable,  $Q_k$ ) and to strength ( $f_y$ ) are additionally indicated, for the OSs of Table 3.

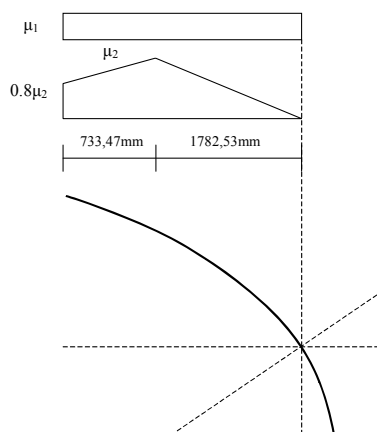


Fig. 7. Snow condition for the parabola when the solar collector is rotated to the safety position.

Combinations		$G_k$	$Q_{1k}$ (wind)	$Q_{2k}$ (snow)	$f_y$
$W_130$	$W_130R$	1.	1.	0.	1.
$W_260$	$W_260R$	1.	1.	0.	1.
$W_3\alpha$ $-120^\circ \leq \alpha \leq 75^\circ$ (Table 3)	$W_3\alpha E$	1.4*	1.5	0.	1.
$W_4\beta ; \beta = 0^\circ$ (Table 3)	$W_4\beta E$	1.4*	1.5	0.	1.
$W_4\beta ; \beta = -120^\circ$ (Table 3)	$W_4\beta E$	1.4*	1.5	0.	1.
		1.4*	1.5	1.05	1.
		1.4*	1.05	1.5	1.
		1.4*	0.	1.5	1.
	$W_4\beta P$	1.4*	1.5	1.05	0.83
		1.4*	1.05	1.5	0.83

Table 7. Main load combinations and corresponding multiplicative coefficients (\*: if not acting in favour of safety; R: rare; E: elastic limit state; P: plastic collapse).

Particularly, for combinations related to states  $W_130$  ( $W_1, 30^\circ$ ) and  $W_260$ , just *rare* ones are considered, being *frequent* and *quasi-permanent* combinations already included.

In the following, the main results related only to the concentration system are reported, being the conducted design and analysis methodology repeatable in the same way to the other macro-systems, i.e. the torque system and the module's support.

## 6. Analysis and verification of the concentration system

The concentration system is composed by three main elements: centering, stringers and reflecting mirrors (Figures 8 and 9). The system has been analysed considering a single modulus of 12 m, reproducing also the torque tube to which the centerings are linked.

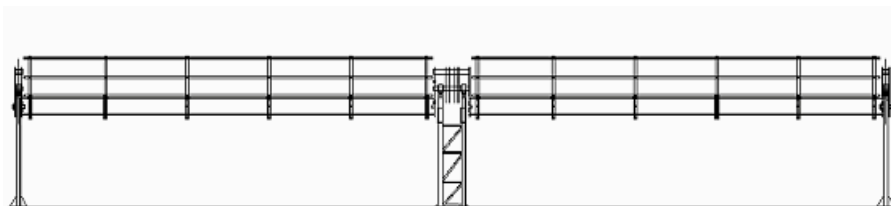


Fig. 8. Sketch of the solar collector (portion).

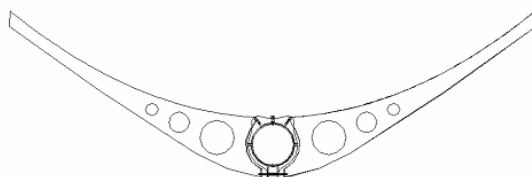


Fig. 9. Sketch of a typical centering (first proposal).

### 6.1 Limit states and load combinations

As already reported in the previous Section, the considered limit states and load combinations are summarized in Table 8. Correspondingly, OSs  $W_1$  and  $W_2$  are associated to SLSs for which the wind loads refer to a medium velocity and the serviceability limits referring to maximum torsion and maximum deformation, respectively, must be verified. Differently, in the ULSs  $W_3$  and  $W_4$  the structural permanence within the elastic state as well as tightness under loads corresponding to a characteristic peak wind must be verified. Particularly, in the  $W_4$  state the possible presence of snow has to be additionally accounted for. For both ULSs, a structural instability verification has to be conducted.

Operational states	$V_{ref}$ (m/s) @10m	Limit state	Reference velocity
$W_1$	7	Serviceability	Medium
$W_2$	14	Serviceability	Medium
$W_3$	21	Ultimate, Elastic	Peak
$W_4$	28	Ultimate, Collapse	Peak

Table 8. Summary of adopted limit states and load combinations for the concentration system.

In Table 9 all the possible load combinations are shown which have been considered for developing the above-mentioned verifications. It is to be noticed that, for the collapse ULS, in addition to the combinations required by the Recommendations, two other combinations have been evaluated in which the snow and the wind alone are present: this was necessarily done due to the fact that the concurrent presence of the two loads, if from one side it increases the acting forces, from the other it reduces the magnitude of the torque bending, so

reducing the stress state in some fundamental structural components. All the analyses have been performed in an elastic state and just in those cases, corresponding to a collapse ULS, in which the structure is particularly stressed, a tightness evaluation within a plastic state has been conducted.

<i>LS</i>	<i>OS</i>	<i>Angle</i> (°)	<i>G_receiver</i>	<i>G_conc</i>	<i>Q_wind</i>	<i>Q_snow</i>	<i>c_G</i>	<i>c_Qv</i>	<i>c_Qn</i>	<i>f<sub>y</sub></i>	<i>ID</i>		
ELS	W <sub>1</sub>	30	yes	yes	yes	no	1.00	1.00	0.00	1.00	w1p030c1		
ELS	W <sub>2</sub>	60	yes	yes	yes	no	1.00	1.00	0.00	1.00	w2p060c1		
ULS elastic	W <sub>3</sub>	75	yes	yes	yes	no	1.40	1.50	0.00	1.00	w3p075c1		
							1.00	1.50	0.00	1.00	w3p075c2		
		60	yes	yes	yes	no	1.40	1.50	0.00	1.00	w3p060c1		
							1.00	1.50	0.00	1.00	w3p060c2		
		30	yes	yes	yes	no	1.40	1.50	0.00	1.00	w3p030c1		
							1.00	1.50	0.00	1.00	w3p030c2		
		0	yes	yes	yes	no	1.40	1.50	0.00	1.00	w3p000c1		
							1.00	1.50	0.00	1.00	w3p000c2		
		-30	yes	yes	yes	no	1.40	1.50	0.00	1.00	w3m030c1		
							1.00	1.50	0.00	1.00	w3m030c2		
		-120	yes	yes	yes	no	1.40	1.50	0.00	1.00	w3m120c1		
							1.00	1.50	0.00	1.00	w3m120c2		
		ULS collapse	W <sub>4</sub>	-120	yes	yes	yes	load1	1.40	1.50	1.05	0.83	w4m120c1
									1.00	1.50	1.05	0.83	w4m120c2
1.40	1.05								1.50	0.83	w4m120c3		
1.00	1.05								1.50	0.83	w4m120c4		
1.40	1.50								0.00	0.83	w4m120c5		
1.00	1.50								0.00	0.83	w4m120c6		
1.40	0.00								1.50	0.83	w4m120c7		
1.00	0.00								1.50	0.83	w4m120c8		
-120	yes			yes	yes	load2	1.40	1.50	1.05	0.83	w4m120c9		
							1.00	1.50	1.05	0.83	w4m120c10		
							1.40	1.05	1.50	0.83	w4m120c11		
							1.00	1.05	1.50	0.83	w4m120c12		
							1.40	1.50	0.00	0.83	w4m120c5		
							1.00	1.50	0.00	0.83	w4m120c6		
							1.40	0.00	1.50	0.83	w4m120c13		
							1.00	0.00	1.50	0.83	w4m120c14		
0	yes			yes	yes	no	1.40	1.50	0.00	0.83	w4p000c1		
							1.00	1.50	0.00	0.83	w4p000c2		

Table 9. Details of the load combinations for the concentration system.

## 6.2 Analysis methodologies.

The structural element has been studied through the F.E. Cast3M code, realizing a 3D model of the 12 m concentration system (Figure 10). Reflecting mirrors, centerings, stringers, torque tube and edge plates. Apart from the plates, which have been modelled through infinitely-rigid beams, all the other components, being made by thin plates, have been modelled through 2D shell elements, able to take into account membrane as well as bending and shear stresses.

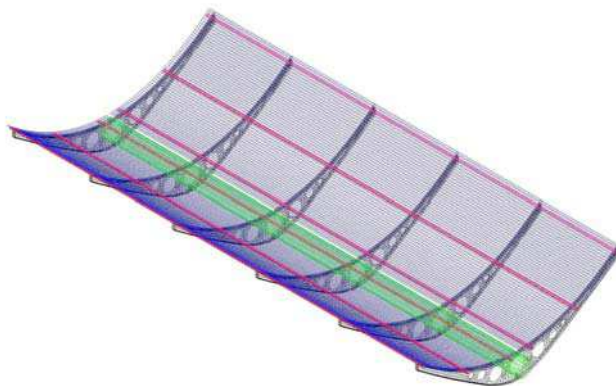


Fig. 10. 3D F.E. model of the concentration system.

The global structural constraints, applied to the edges of the connecting plates, have been applied such to create an isolated and isostatic system, so the stress state doesn't change due to possible loads transmitted by the adjacent moduli.

## 6.3 Discussion of the main numerical results.

The main results referring to SLSs for weak and medium wind, as well as to ULSs (elastic and collapse) are depicted in Table 10; stresses are calculated as the maximum equivalent Tresca stress,  $F_{saf}$  is the safety factor obtained by dividing the material yield limit (reduced in case of ULS, see Tables 7 and 9) by the above stress. The medium value of the parabola's deformation is additionally reported (which is always lower than  $\pm 5$  mm, the assumed limit within SLSs).

It is hence evidenced that in both elastic and collapse ULSs the safety factors are generally lower than one; by examining the results in more detail, it has been found that local yielding occur in the higher and middle part of the centering and in some zones connecting the centering with the stringers.

Anyway, it is to be said that the model has been developed to study the global stress level in the various components and not to locally analyse the connecting constructive details which need specific 3D models; a possible local overcome in the stress yield limit and/or consequent re-distributions of stresses can't be caught by such an approach, as explained below.

For sake of brevity, the contour maps of stresses have been included (Figures 11 and 12) referring only to w3p060c1 and w4m120c9 combinations: it is here evidenced the much localized nature of plasticization, as explained above.



	Component	$\sigma_{max}$	$F_{tar}$	$\Delta$ (mm)		Component	$\sigma_{max}$	$F_{tar}$
w1p030c1	Stringers	87	3,17	2,33	w4m120c1	Stringers	580	<b>0,47</b>
	Centerings	108	2,54			Centerings	564	<b>0,49</b>
w2p030c0	Stringers	120	2,29	3,66	w4m120c2	Stringers	570	<b>0,48</b>
	Centerings	148	1,86			Centerings	540	<b>0,51</b>
w2p060c1	Stringers	117	2,36	3,05	w4m120c3	Stringers	453	<b>0,61</b>
	Centerings	142	1,94			Centerings	494	<b>0,56</b>
w3p075c1	Stringers	545	<b>0,51</b>	w4m120c4	Stringers	442	<b>0,62</b>	
	Centerings	597	<b>0,46</b>		Centerings	470	<b>0,59</b>	
w3p075c2	Stringers	542	<b>0,51</b>	w4m120c5	Stringers	532	<b>0,52</b>	
	Centerings	578	<b>0,48</b>		Centerings	500	<b>0,55</b>	
w3p060c1	Stringers	571	<b>0,48</b>	w4m120c6	Stringers	522	<b>0,53</b>	
	Centerings	622	<b>0,44</b>		Centerings	505	<b>0,54</b>	
w3p060c2	Stringers	563	<b>0,49</b>	w4m120c7	Stringers	237	1,16	
	Centerings	602	<b>0,46</b>		Centerings	333	<b>0,83</b>	
w3p030c1	Stringers	549	<b>0,50</b>	w4m120c8	Stringers	210	1,31	
	Centerings	604	<b>0,46</b>		Centerings	298	0,92	
w3p030c2	Stringers	534	<b>0,51</b>	w4m120c9	Stringers	615	<b>0,45</b>	
	Centerings	566	<b>0,49</b>		Centerings	639	<b>0,43</b>	
w3p000c1	Stringers	239	1,15	w4m120c10	Stringers	605	<b>0,45</b>	
	Centerings	262	1,05		Centerings	615	<b>0,45</b>	
w3p000c2	Stringers	214	1,29	w4m120c11	Stringers	531	<b>0,52</b>	
	Centerings	232	1,19		Centerings	612	<b>0,45</b>	
w3m030c1	Stringers	218	1,26	w4m120c12	Stringers	524	<b>0,53</b>	
	Centerings	221	1,24		Centerings	577	<b>0,48</b>	
w3m030c2	Stringers	217	1,27	w4m120c13	Stringers	392	<b>0,70</b>	
	Centerings	183	1,50		Centerings	490	<b>0,56</b>	
w3m120c1	Stringers	316	<b>0,87</b>	w4m120c14	Stringers	386	<b>0,71</b>	
	Centerings	299	<b>0,92</b>		Centerings	454	<b>0,61</b>	
w3m120c2	Stringers	305	<b>0,90</b>	w4p000c1	Stringers	357	<b>0,77</b>	
	Centerings	285	<b>0,97</b>		Centerings	383	<b>0,72</b>	
w4m120c1	Stringers	580	<b>0,47</b>	w4p000c2	Stringers	332	<b>0,83</b>	
	Centerings	564	<b>0,49</b>		Centerings	353	<b>0,78</b>	
w4m120c2	Stringers	570	<b>0,48</b>					
	Centerings	540	<b>0,51</b>					
w4m120c3	Stringers	453	<b>0,61</b>					
	Centerings	494	<b>0,56</b>					

Table 10. Numerical results (static analyses) for the concentration system.

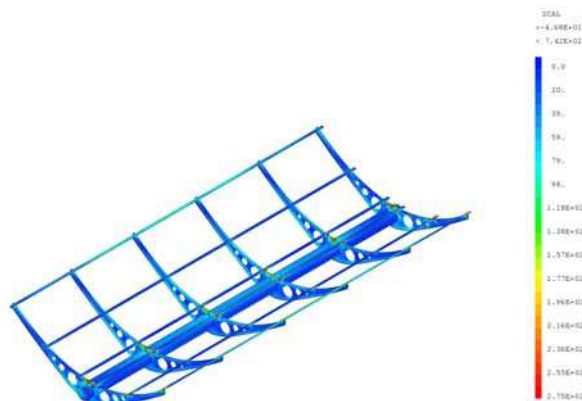


Fig. 11. Contour map of maximum equivalent Tresca stresses for w3p060c1.

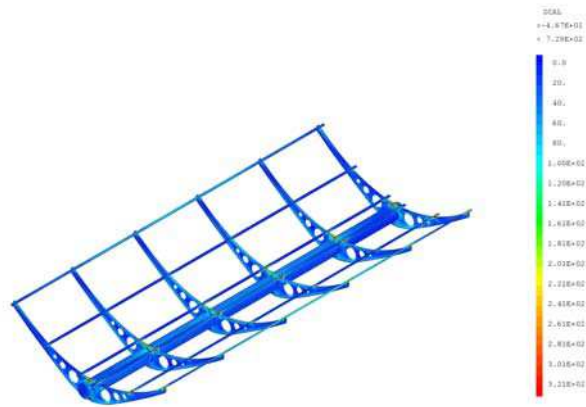


Fig. 12. Contour map of maximum equivalent Tresca stresses for w4m120c9.

The 3D static analyses revealed an appropriate response of the structure under a variety of actions and once, for example, the material strength had been locally overcome, appropriate design procedures have been updated and nonlinear (for material and geometry) analyses performed (see e.g. Figure 13).

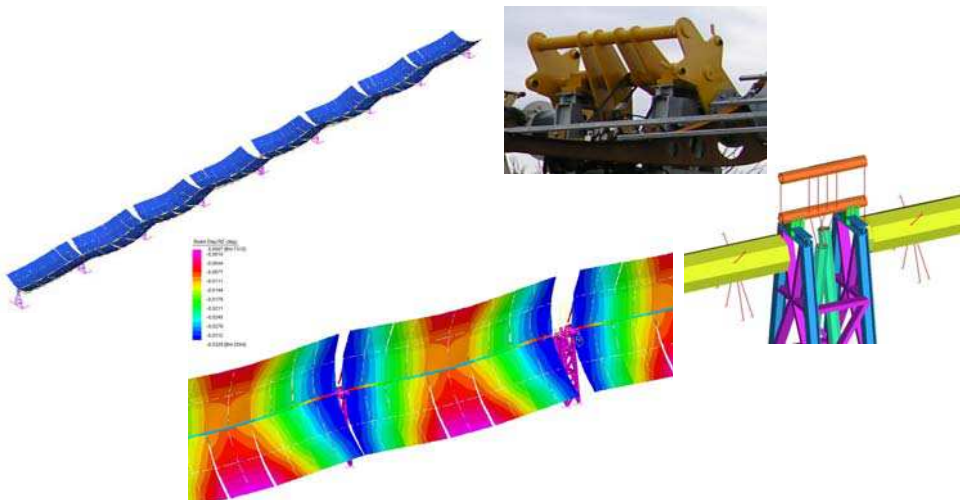


Fig. 13. Typical results from modal and seismic analyses and scheme for a modelled joint.

Additional modal, spectral and generally dynamic analyses have been conducted for the whole CSP system (see Figure 14) to understand the global structural behaviour and to newly upgrade the first design sketch.

The discussion about such results and the corresponding structural response can't be reported here for sake of brevity.

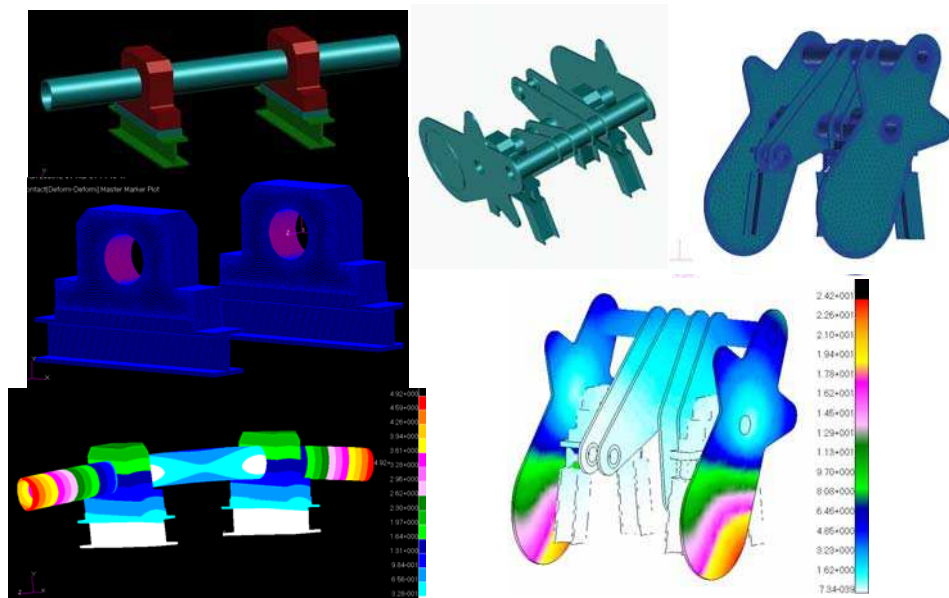


Fig. 14. Joints, pins and specific nodes studied through 3D nonlinear analyses for material and geometry to test their effective structural response and to verify the requirements of the different operational states.

## 7. Description of heat storage concrete systems

The main advantage of thermal solar power plants is the possibility to use relatively economical storage systems, if compared to other renewable energies (i.e. photo-voltaic and wind). Storing electricity is much more expensive than storing thermal energy itself. Thermal Energy Storage (TES) option can collect energy in order to shift its use to later times, or to smooth out the plant output during irregularly cloudy weather conditions. Hence, the functional operativeness of a solar thermal power plant can be extended beyond periods of no solar radiation without the need of burning fossil fuel. Periods of mismatch among energy supplied by the sun and energy demand can be reduced. Economic thermal storage is a technological key issue for the future success of solar thermal technologies.

In our days, among eight thermal storage systems in thermo-electric solar plants, seven have been of experimental or prototypal nature and only one has been a commercial unit (Salomoni et al., 2008). All the considered systems are "at sensible heat storage": two single-tanks oil thermo-cline systems, four two-tanks single medium systems (one oil- and three molten salt-) and two single-tanks double medium systems. Actually the most advanced technology for heat storage in solar towers and through collector plants considers the use of a two-tanks molten salt system (Ives et al., 1985).

Generally, the hot and cold tanks are located on the ground and they are characterized by an internal circumferential and longitudinally-wrinkled liner, appropriately thermally insulated. The cost of the liner is the primary cost of such a tank. In recent studies it has been shown that an increase in the hourly capacity accumulation reduces sensibly the cost of the

produced electrical energy (LEC); this leads to increase the reservoir dimensions from the 11.6 m diameter and 8.5 m height of the Solar Two power plant to the larger 18.9 m diameter and 2.5 height calculated in the Solar Tres power plant design phase.

Already in 1985, the Solar Energy Research Institute (SERI) commissioned the conceptual design of a below-grade cone shape storage (Figure 15) with 900°C molten carbonate salts (Copeland et al., 1984). This solution, even though interesting because of the use of low cost structural materials, showed some limits connected to the high level of corrosion induced by carbonate and high temperature.

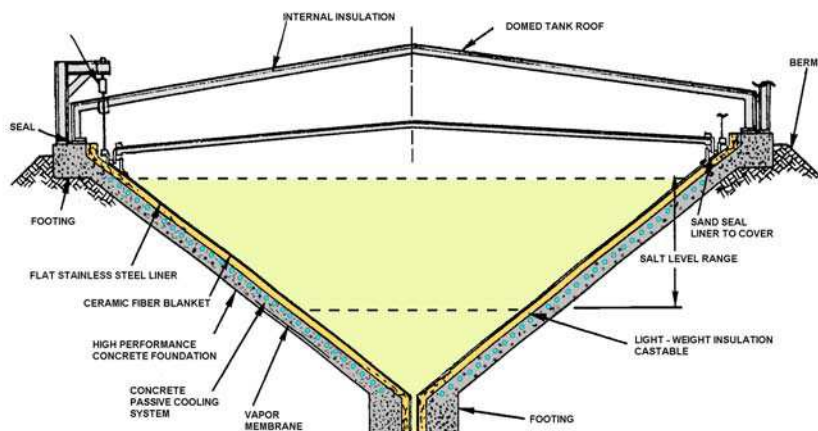


Fig. 15. Conical storage partially buried in the ground.

Such a type of storage is here reconsidered in combination with nitrate molten salts at a maximum temperature of 565°C, using an innovative high performance concrete (HPC) for the tanks. From the technological point of view, the innovations rely in:

- higher structural safety related to the reduced settlements;
- employment of HPC containment structures and foundations characterised by lower costs with respect to stainless steel structures;
- substitution of highly expensive corrugated steel liners with plane liners taking advantage of the geometric compensation of thermal dilations due to the conical shape of the tank;
- possibility of employing freezing passive systems for the concrete basement made of HPC, able to sustain temperature levels higher than those for OPC;
- fewer problems when the tank is located on low-strength soils.

The planned research activities required the upgrade of a F.E. coupled model for heat and mass transport (plus mechanical balance) to estimate concrete tanks durability under prolonged thermal loads and cyclic temperature variations due to changes in the salts level. The presence of a surrounding soil volume is additionally accounted for to evaluate environmental risk scenarios.

### 7.1 Mathematical-numerical modeling of concrete

Concrete is treated as a multiphase system where the voids of the skeleton are partly filled with liquid and partly with a gas phase (Baggio et al., 1995; Gawin et al., 1999). The liquid

phase consists of bound water (or adsorbed water), which is present in the whole range of water contents of the medium, and capillary water (or free water), which appears when water content exceeds so-called solid saturation point  $S_{ssp}$  (Couture et al., 1996), i.e. the upper limit of the hygroscopic region of moisture content. The gas phase, i.e. moist air, is a mixture of dry air (non-condensable constituent) and water vapour (condensable gas), and is assumed to behave as an ideal gas.

The approach here is to start from a phenomenological model (Schrefler et al., 1989; Majorana et al., 1997; Majorana et al., 1998; Majorana & Salomoni, 2004 (b); Salomoni et al., 2007 (a)), originally developed by Bažant and co-authors, e.g. (Bažant, 1975; Bažant & Thonguthai, 1978; Bažant & Thonguthai, 1979; Bažant et al., 1988), in which mass diffusion and heat convection-conduction equations are written in terms of relative humidity, to an upgraded version in which its non-linear diffusive nature is maintained as well as the substitution of the linear momentum balance equations of the fluids with a constitutive equation for fluxes, but new calculations of thermodynamic properties for humid gases are implemented too to take into account different fluid phases as well as high ranges of both pressure and temperature. Additionally, Darcy's law is abandoned when describing gas flow through concrete.

The proposed model couples non-linear geometric relations with empirical relations; to enhance its predictive capabilities, a predictor-corrector procedure is supplemented to check the exactness of the solution. For additional details the reader is referred to (Salomoni et al., 2007 (b); Salomoni et al., 2008; Salomoni et al., 2009).

## 7.2 Numerical analyses

A conical tank for storing hot salts has been modelled through the F.E. research code NEWCON3D (Figure 16) using 330 8-node isoparametric elements (axis-symmetric condition). In agreement with the design criteria, it is proposed to employ a High Performance Concrete (HPC), particularly a C90 for this analysis, to increase both the operational temperature up to 120°C -against the usual 90°C for ordinary concretes- and concrete durability. The whole tank is composed by a flat stainless steel liner in contact with the salts and a ceramic fibre blanket (not modelled here) close to the concrete main structure (Figure 15). An additional passive cooling system is supposed to be added within the concrete thickness to reach such operational temperature on concrete surfaces. Geometric details have not been included for privacy reasons.

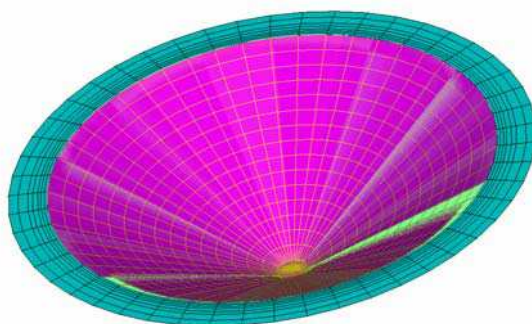


Fig. 16. F.E. discretization for the thermal storage concrete tank.

The adopted material properties are listed in Table 11.

Water/cement ratio	0.29
Elastic modulus [MPa]	$0.367 \cdot 10^5$
Poisson's ratio	0.18
Reference diffusivity along x/y directions [mm <sup>2</sup> /day]	$0.1 \cdot 10^2$
Intrinsic liquid permeability [mm <sup>2</sup> ]	$2.0 \cdot 10^{-19}$
Unrestrained shrinkage for $h = 0$ ( $\epsilon_{sh}$ )	$-0.4 \cdot 10^{-2}$
Thermal expansion coefficient of solid	$0.12 \cdot 10^{-4}$
Hygro-thermal coefficient	$0.5 \cdot 10^{-2}$
Thermal capacity [N/(mm <sup>2</sup> K)]	2.0
Heat conductivity along x/y directions [N/(day K)]	$0.18144 \cdot 10^6$
Coefficient $\alpha_0$ for diffusivity	$0.5 \cdot 10^{-1}$

Table 11. Material parameters for concrete C90.

The concrete tank is subjected to transient heating from the internal side assuming to reach the maximum temperature of 100°C in 8 days; the concrete tank has initially a relative humidity of 60% and a temperature of 30°C. In the first analyses (pushed up to about 4 months) the tank is supposed to be simply supported on its basement only.

The results in terms of R.H. (a) and temperature (b) are presented in Figure 17 (3D plot): the development of the R.H. bowl in time (along a typical tank section) is clearly evident; the peaks in R.H. for the zone closest to the heated surface are not referable to the phenomenon of “moisture-clog” (Majorana et al., 1998; Chung et al., 2006), because of the limited value of the temperature gradient, but anyway it is driven by the coupling between humidity and temperature fields and it is connected to the low intrinsic liquid permeability of the adopted HPC. Once 100°C has been reached, concrete starts depleting itself of water, thereby making the relative humidity values tend towards zero (but very slowly: in fact, after about 4 months, a concrete thickness of about 255 mm is still in saturated conditions).

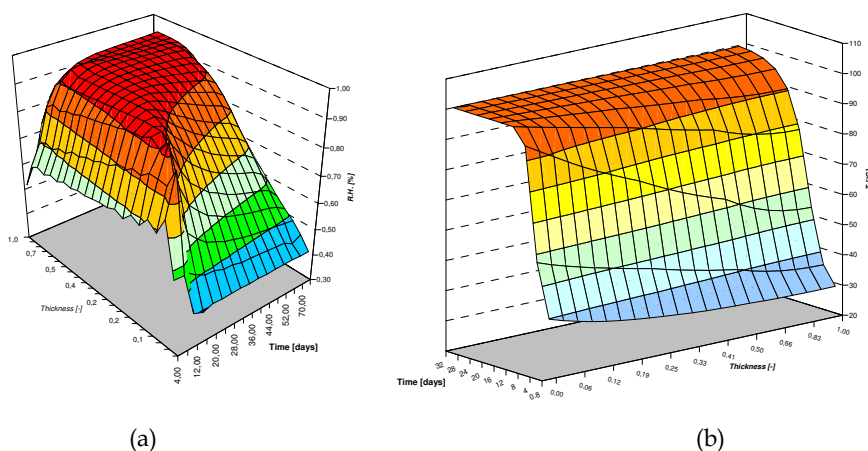


Fig. 17. R.H. (a) and temperature (b) time-history along a typical tank section.



The desaturation occurring within the concrete tank is mainly caused by the evaporation of water, resulting in formation of a zone of increased vapour pressure. Vapour pressure gradients cause vapour flow towards both the heated surface and the external side of the tank. Moreover, the existing temperature gradient causes thermo-diffusion of water vapour towards the colder layer of the wall. These vapour flows result in an increase in R.H. above its initial value as well as in condensation of vapour in the colder layers and subsequent slight increase in saturation.

The effect of a surrounding ground volume (dry sand) has been additionally evaluated on the development of the thermal front up to 2 years; the main results are here recalled (Salomoni et al., 2008): if considering a sand with a specific heat of 781.25 J/(kg K) and a thermal conductivity of 0.35 W/(m K), a shift the maximum temperature to farther times is revealed with respect to the results obtained from the analysis for the tank only. Additionally, the peak of 100°C seems to be not reachable even after several months.

The situation is clearly preferable when considering the durability performances of the concrete tank, but anyway the heat level is again not admissible for the soil: under such temperatures chemical reactions can take place if organic materials are present, even if a soil treatment is usually performed; moreover, a desiccation of zones around the tank combined with possible re-wettings due to rainfalls could induce relative displacements and consequently tank movements. Hence, being the hypothesis of an additional cooling system (or an additional foundation) too expensive in the design of such structures, it should be planned to use gravelly soils when preparing the surrounding embankment.

## 8. Conclusions

This Chapter gives a general view related to the last experiences R&D in the field of new technologies for solar energy exploitation within the Italian context, directly exportable abroad due to the followed design and analysis methodologies. The main structures and elements characterizing a solar power plant with parabolic-trough solar concentrators and a double-tank below ground system are studied, evidencing the fundamental design and modelling results.

From the process of analysis and verification of a 100 m parabolic trough solar concentrator, with reference to each system, subsystem and construction details, some remarks can be evidenced. Within this design approach, four operational states corresponding to different design winds, i.e.  $W_1 = 7$  km/h,  $W_2 = 14$  km/h,  $W_3 = 21$  km/h e  $W_4 = 28$  km/h, have been defined, to which two SLSs (for medium wind) and two ULSs (for peak wind) are respectively associated. Then, considering that the snow load acts simultaneously with the self-weight and with some probability contemporaneously with the wind load, the following conclusions can be stated:

- *Concentration system*: the adoption of a 3D FE model, corresponding to a 12 m module, has been considered as adequate to perform such a design and verification procedure. Safety or functioning problems have not been evidenced in the SLSs, linked to the operational states with  $W_1$  and  $W_2$  wind types. With reference to the elastic ULS (ELS), the maximum value for the  $\sigma_{eq}$  has been locally overcome (higher and middle part of the centering and some zones connecting the centering with the frames); such trend has been confirmed in the collapse ULSs.
- *Torque system (omissis)*: the adoption of a simplified 3D FE model, in which the structure is characterized by a series of beams with sections of appropriate bending and torsion

inertias, has been considered as adequate to perform such a design and verification procedure. Safety, functioning and instability problems have not been evidenced in the SLSs, linked to the operational states with  $W_1$  and  $W_2$  wind types. In fact, with reference to the SLS verifications for weak wind, the only imposed constraint is that the maximum rotation of the torque tube is lower than 2 mrad and this constraint is largely satisfied, as well as the displacements requirements (limit of 20 mm for the camber). In relation to the ELS, the only constraint is the maintenance of the structural behaviour within the elastic limits in any condition, as proved by the obtained high safety factors. When the structure is verified under the collapse ULS, collapse must not occur in the standard safety position: two load cases exist for which such requirement is not satisfied and the critical action is given by the snow. Differently, the stability analyses referring to the heaviest load conditions ( $W_3$  and  $W_4$ ) show safety factors always higher than one. As regards the constructive details, the requirement of minimum distances between the connectors and the plates' edges, as indicated by the Eurocode 3, is not satisfied so that appropriate design prescriptions have been planned by the authors.

- *Module's support system (omissis)*: once again a simplified 3D FE model, in which the structure is characterized by a series of beams with sections of appropriate bending and torsion inertias, has been adopted. Both the intermediate and final supports, under SLSs for weak wind, are characterized by low stresses, as well as under SLSs for medium wind. The constraint of a structural behaviour within the elastic range in the elastic ULS is fully respected, as well as the absence of collapse in the standard safety position (collapse ULS). The stability analyses referring to the heaviest load conditions ( $W_3$  and  $W_4$ ) show again safety factors always higher than one.

A series of linear and non-linear static 3D analyses have been followed by modal, spectral and generally dynamic analyses to understand the structural behaviour of the whole CSP system and the first design sketch has been consequently updated. The analyses revealed an appropriate response of the whole structure under a variety of actions and once, e.g., the material strength had been locally overcome, local non-linear analyses have been conducted and the constructive details eventually re-designed.

Additionally, within the medium temperature field, an innovative approach has been presented for the conceptual design of liquid salts concrete storage systems. A multi-tank sensible-heat storage system has been proposed for storing thermal energy, with a two-tanks molten salt system. The hygro-thermal behaviour of a HPC tank has been assessed through a coupled F.E. code based on the theory by Bažant and enhanced by additional constitutive and thermodynamic relationships. A predictor-corrector procedure has been included to check the exactness of the solution. The study allows for estimating the durability performances of the tank: after about one month, all the structure is fully heated, possibly inducing thermal damage within concrete; such a result is slightly modified when modelling the domain more in detail, i.e. tank plus surrounding ground, or when changes in the salts level are considered. Even if at present some geometric and mechanical characteristics are still to be fixed, so that they can consequently induce an unavoidable uncertainty on the numerical results, the generality of the approach is not affected by such restrictions, and the results themselves can be evaluated as first guidelines in defining design criteria for liquid salts concrete systems. In fact, this study is the first step in a new research field and is being extended within the Italian Research Project "Elioslab - Research Laboratory for Solar Technologies at High Temperatures" started at the end of 2007.



Again, independently on the specificity and interest of the application, it has been shown here that the fully coupled mathematical-numerical model proposed (whose details have been reported for the hygro-thermal field only and whose predictive abilities have already been demonstrated in (Salomoni et al., 2007) even if in its not-upgraded form) has been enhanced through additional thermodynamic and constitutive relationships, allowing for obtaining more complete results in terms of water vapour pressure, gas pressure and capillary pressure which become fundamental variables mainly when higher temperature regimes are to be considered.

## 9. References

- Antonaia, A.; Avitabile, M.; Calchetti, G.; Crescenzi, T.; Cara, G.; Giannuzzi, G.M.; Maccari, A.; Miliozzi, A.; Rufoloni, M.; Prischich, D.; Vignolini, M. (2001). Design sketch of the parabolic trough collector for solar plants. *ENEA/TM/PRES/2001\_09*, Rome, Italy (technical report, in Italian).
- Baggio, P.; Majorana, C.E.; Schrefler, B.A. (1995). Thermo-hygro-mechanical analysis of concrete. *International Journal for Numerical Methods in Fluids*, Vol. 20, 573-595.
- Bažant, Z.P. (1975). Pore pressure, uplift, and failure analysis of concrete dams. *Int. Commission on Large Dams*, Swansea, UK.
- Bažant, Z.P.; Thonguthai, W. (1978). Pore pressure and drying of concrete at high temperature. *Journal of the Engineering Materials Division, ASME*, Vol. 104, 1058-1080.
- Bažant, Z.P.; Thonguthai, W. (1979). Pore pressure in heated concrete walls: theoretical predictions. *Magazine of Concrete Research*, Vol. 31, No.107, 67-76.
- Bažant, Z.P.; Chern, J.C.; Rosenberg, A.M.; Gaidis, J.M. (1988). Mathematical Model for Freeze-Thaw Durability of Concrete. *Journal of the American Ceramic Society*, Vol. 71, No. 9, 776-83.
- Chung, J.H.; Consolazio, G.R.; McVay, MC. (2006). Finite element stress analysis of a reinforced high-strength concrete column in severe fires. *Computers and Structures*, Vol. 84, 1338-1352.
- Copeland, R.J.; West, R.E.; Kreith, F. (1984). Thermal Energy Storage at 900°C. *Proc. 19<sup>th</sup> Ann. Intersoc. Energy Conversion Engrg. Conf.*, San Francisco, Aug. 19-24, 1171-1175.
- Couture, F.; Jomaa, W.; Ruiggali, J.R. (1996). Relative permeability relations: a key factor for a drying model. *Transport in Porous Media*, Vol. 23, 303-335.
- ENEA (2003). <http://www.enea.it/com/ingl/solarframe.htm>.
- Gawin, D.; Majorana, C.E.; Schrefler, B.A. (1999). Numerical analysis of hygro-thermal behaviour and damage of concrete at high temperature. *Mechanics of Cohesive-Frictional Materials*, Vol. 4, 37-74.
- Giannuzzi, G.M.; Majorana, C.E.; Miliozzi, A.; Salomoni, V.A.L.; Nicolini, D. (2007) Structural design criteria for steel components of parabolic-trough solar concentrators. *Journal of Solar Energy Engineering*, Vol. 129, 382-390.
- Herrmann, U.; Kelly, B.; Price, H. (2004). Two-tank molten salt storage for parabolic trough solar power plants. *Energy*, Vol. 29, No. 5-6, 883-893.
- Ives, J.; Newcomb, J.C.; Pard, A.G. (1985). High Temperature Molten Salt Storage. *SERI/STR-231-2836* (technical paper).

- Majorana, C.E.; Salomoni, V.; Secchi, S. (1997). Effects of mass growing on mechanical and hygrothermic response of three-dimensional bodies. *Journal of Materials Processing Technology*, PRO064/1-3, 277-286.
- Majorana, C.E.; Salomoni, V.; Schrefler, B.A. (1998). Hygrothermal and mechanical model of concrete at high temperature. *Materials and Structures*, Vol. 31, 378-386.
- Majorana, C.; Salomoni, V. (2004) (a). Selection, elaboration and application of recommendations for designing parabolic trough solar concentrators. Functional description, classification and selection of design codes for their structural elements. *Report ENEA-TRASTEC*, Rome-Padua, Italy (in Italian).
- Majorana, C.; Salomoni, V. (2004) (b). Parametric analyses of diffusion of activated sources in disposal forms. *Journal of Hazardous Materials*, A113, 45-56.
- Majorana, C.; Salomoni, V. (2005) (a). Design guide for parabolic trough solar concentrators. *Report ENEA-TRASTEC*, Rome-Padua, Italy (in Italian).
- Majorana, C.; Salomoni, V. (2005) (b). Analyses and structural verifications for a 100 m-parabolic trough solar concentrator. *Report ENEA-TRASTEC*, Rome-Padua, Italy (in Italian).
- Miliozzi, A.; Nicolini, D.; Giannuzzi, G.M. (2007). Evaluation of wind action on parabolic trough concentrators for a high temperature solar plant. *Enea Report RT/2007/13/TER* (in Italian).
- Pilkington Solar International GmbH (2000). Survey of Thermal Storage for Parabolic-Trough Power Plants, *NREL/SR-550-27925* (technical report).
- Rubbia, C.; and ENEA Working Group (2001). Solar thermal energy production: guidelines and future programmes of ENEA. *ENEA/TM/PRES/2001\_7*, Rome, Italy (technical report).
- Salomoni, V.A.; Giannuzzi, G.M.; Majorana, C.E.; Miliozzi, A.; Nicolini, D. (2006). Structural design of parabolic-trough solar concentrators' steel components against wind and natural hazards, *Proceedings of the 3<sup>rd</sup> Int. Conf. on Protection of Structures Against Hazards* (Majorana, Salomoni, Lok Eds.), Venice, Italy, sept. 28-29 (ISBN 981-05-5561-X) (keynote lecture).
- Salomoni, V.A.; Mazzucco, G.; Majorana, C.E. (2007) (a). Mechanical and durability behaviour of growing concrete structures. *Engineering Computations*, Vol. 24, No. 5, 536-561.
- Salomoni, V.A.; Majorana, C.E.; Khoury, G.A. (2007) (b). Stress-strain experimental-based modeling of concrete under high temperature conditions. In: B.H.V. Topping (Ed.), *Civil Engineering Computations: Tools and Techniques*, Ch. 14, Saxe-Coburg Publications, 319-346.
- Salomoni, V.A.; Majorana, C.E.; Giannuzzi, G.M.; Miliozzi, A. (2008) Thermal-fluid flow within innovative heat storage concrete systems for solar power plants. *International Journal of Numerical Methods for Heat and Fluid Flow* (Special Issue), Vol. 18(7/8), 969-999.
- Salomoni, V.A.; Majorana, C.E.; Mazzucco, G.; Xotta, G.; Khoury, G.A. (2009). Multiscale Modelling of Concrete as a Fully Coupled Porous Medium. In: J.T. Sentowski (Ed.), *Concrete Materials: Properties, Performance and Applications*, Ch. 3, NOVA Publishers, 2009 (in press).
- Schrefler, B.A.; Simoni, L.; Majorana, C.E. (1989). A general model for the mechanics of saturated-unsaturated porous materials. *Materials and Structures*. Vol. 22, 323-334.



## **Solar Energy**

Edited by Radu D Rugescu

ISBN 978-953-307-052-0

Hard cover, 432 pages

**Publisher** InTech

**Published online** 01, February, 2010

**Published in print edition** February, 2010

The present "Solar Energy" science book hopefully opens a series of other first-hand texts in new technologies with practical impact and subsequent interest. They might include the ecological combustion of fossil fuels, space technology in the benefit of local and remote communities, new trends in the development of secure Internet Communications on an interplanetary scale, new breakthroughs in the propulsion technology and others. The editors will be pleased to see that the present book is open to debate and they will wait for the readers' reaction with great interest. Critics and proposals will be equally welcomed.

### **How to reference**

In order to correctly reference this scholarly work, feel free to copy and paste the following:

Valentina A. Salomoni, Carmelo E. Majorana, Giuseppe M. Giannuzzi, Adio Miliozzi and Daniele Nicolini (2010). New Trends in Designing Parabolic trough Solar Concentrators and Heat Storage Concrete Systems in Solar Power Plants, *Solar Energy*, Radu D Rugescu (Ed.), ISBN: 978-953-307-052-0, InTech, Available from: <http://www.intechopen.com/books/solar-energy/new-trends-in-designing-parabolic-trough-solar-concentrators-and-heat-storage-concrete-systems-in-so>

# **INTECH**

open science | open minds

### **InTech Europe**

University Campus STeP Ri  
Slavka Krautzeka 83/A  
51000 Rijeka, Croatia  
Phone: +385 (51) 770 447  
Fax: +385 (51) 686 166  
[www.intechopen.com](http://www.intechopen.com)

### **InTech China**

Unit 405, Office Block, Hotel Equatorial Shanghai  
No.65, Yan An Road (West), Shanghai, 200040, China  
中国上海市延安西路65号上海国际贵都大饭店办公楼405单元  
Phone: +86-21-62489820  
Fax: +86-21-62489821

© 2010 The Author(s). Licensee IntechOpen. This chapter is distributed under the terms of the [Creative Commons Attribution-NonCommercial-ShareAlike-3.0 License](#), which permits use, distribution and reproduction for non-commercial purposes, provided the original is properly cited and derivative works building on this content are distributed under the same license.